THE ASTROPHYSICAL JOURNAL SUPPLEMENT SERIES, 100:149–157, 1995 September

ON THE ELECTRONIC STRUCTURE OF SMALL CARBON GRAINS OF ASTROPHYSICAL INTEREST

V. MENNELLA,[1] L. COLANGELI,[1] E. BUSSOLETTI,[2] G. MONACO,[2] P. PALUMBO,[3] AND A. ROTUNDI[3]
Received 1994 November 29; accepted 1995 February 25

ABSTRACT

In a previous paper Mennella et al. (1995a) studied the evolution of the UV spectrum of small carbon grains due to thermal annealing in the range 250–800°C. The spectral variations were interpreted in terms of internal structural rearrangement of the grains caused by hydrogen loss. The electronic transitions ($\sigma-\sigma^*$ and $\pi-\pi^*$) of the sp^2 clusters forming the grains were indicated as the major factors responsible for determining their extinction properties.

In this paper we present the results of new measurements aimed at probing the heat-induced structural changes. The thermal evolution of the optical gap and of the Raman spectrum, both sensitive to the sp^2 clustering degree, confirms that the observed spectral changes do depend on structural variations. In fact, the π electron delocalization of the sp^2 clusters determines a link between structural and electronic properties in carbons.

We find a basic correlation between the UV peak position and the optical gap. It is interpreted in terms of a dependence of the dipole matrix momentum of π transitions on the sp^2 cluster size.

The attribution of the spectral changes to the grain internal structure is corroborated by morphological analyses. Scanning and transmission electron microscope images show that the fluffy structure of the samples as well as the dimension and the shape of the single grains do not change after the annealing process.

In the astrophysical context, the present results can be relevant for the attribution of the 217.5 nm feature, as they show that the internal structure of carbon grains, having sizes similar to those expected for the "bump" carriers, controls the interaction with UV photons.

Subject headings: circumstellar matter — dust, extinction — methods: laboratory — stars: carbon — ultraviolet: ISM

1. INTRODUCTION

Several astronomical observations, spanning from the far-UV to the millimeter spectral regions, indicate the presence of carbon-based materials in space. Many candidates, such as amorphous carbon grains, coals, graphite particles, and polycyclic aromatic hydrocarbons (PAHs), have been invoked to interpret the observed spectral features. However, the actual nature and the evolution of cosmic carbons still remain uncertain.

One of the most controversial items concerns the attribution of the interstellar extinction bump at 217.5 nm. Although it is commonly assigned to some sort of carbonaceous material, a conclusive attribution has not yet been achieved.

A review of the bump observational properties is reported by Draine (1989). Here, we recall that in diffuse Galactic starlight the scattering albedo decreasing across the feature (Witt et al. 1982) has generally been accepted as evidence that the interstellar bump is due to absorption. Extensive studies of interstellar curves have shown that the peak position, λ_0, is very stable at 217.5 nm along different sight lines, while the full width at half-maximum of the feature, γ, appears smaller in the diffuse cloud medium and larger in dense quiescent regions (Fitzpatrick & Massa 1986). The small λ_0 shifts do not appear correlated with γ variations. Moreover, the bump shape and its intensity are poorly correlated with the extinction rise in the far-UV (Fitzpatrick & Massa 1988).

Since the discovery of the bump, graphite has been suggested as its carrier. Theoretical computations have shown that λ_0 and γ are quite sensitive to the grain size distribution: by increasing the size of small graphite particles, both the parameters increase (Draine & Malhotra 1993).

The observed lack of correlation between λ_0 and γ is a serious difficulty for the graphite hypothesis as stressed by Draine & Malhotra (1993). These authors have analyzed how several grain properties affect the bump profile. They concluded that the observational constraints cannot be satisfied by changes in graphite grain size, shape, clumping, or coating. The profile changes must instead be due to variations in grain dielectric properties caused by impurities, crystallinity degree, or surface effects.

On the other hand, Mathis (1994) has considered that small graphite grains may produce the 217.5 nm extinction feature and attributed the γ variations to their coating. In this simulation, the shape of the graphite spheroidal cores must be closely the same for all sight lines, while the mantles must be characterized by a bulk resonance in the wavenumber range 4.6–5 μm^{-1}. PAH molecules are suggested to have optical properties similar to those required for the mantles. Alternatively, refractory elements such as Fe and Mg might give a major contribution to the mantles. This very specific coating is built "ad hoc" in order to mimic the interstellar bump profile and to reproduce the observed γ variations. Since the coating has dielectric

[1] Osservatorio Astronomico di Capodimonte, via Moiariello, 16, I-80131 Napoli, Italy.
[2] Istituto di Fisica Sperimentale, Istituto Universitario Navale, via A. De Gasperi 5, I-80133 Napoli, Italy.
[3] Dipartimento Ingegneria Aerospaziale, Università degli Studi di Napoli Federico II, Piazzale Tecchio 80, I-80125 Napoli, Italy.

properties very similar to those of the underlying graphitic core, the Mathis model is not totally inconsistent with the conclusions of Draine and Malhotra. In fact, in a rough approximation, this core-mantle structure can be interpreted as a graphitic grain with radially varying dielectric properties.

The above-mentioned results suggest that, at present, the success of theoretical simulations depends on the "fine-tuning" of the carrier's optical properties. Moreover, the difficulty of producing graphite grains in astronomical environments has been pointed out by several authors (Czyzak & Santiago 1973; Donn et al. 1981; Hecht 1986; Mathis & Whiffen 1989). Such an ordered material is unlikely to be formed within the atmosphere of C-rich stars. In fact, the circumstellar extinction of these objects shows a UV bump falling in the wavelength range 230–250 nm, appropriate for amorphous carbon grains (Hecht et al. 1984; Bussoletti et al. 1987; Wright 1989; Muci et al. 1994).

Hecht (1986) outlined an evolution of carbon grains in space and in particular interpreted the 217.5 nm feature as due to a population of small hydrogen-free carbon grains. The dehydrogenation occurs in the diffuse medium because of annealing produced by shock processes and exposure to UV radiation and cosmic rays (Sorrell 1990). The γ variations are caused by differences in grain temperature and impurity content (Hecht 1986) or by the presence of adsorbed hydrogen atoms on the grain surface (Sorrell 1990).

In this context, it appears of primary relevance to probe in the laboratory the structure and the electronic properties of small cosmic analog carbon grains and to investigate their interaction with UV photons. Thermal annealing experiments have indeed shown that the UV spectrum of submicron amorphous carbon grains depends on the hydrogen content (Blanco et al. 1991, 1993). Recently, Mennella et al. (1995a, hereafter Me95) have found that the electronic properties of the sp^2 clusters forming the grains control the UV extinction properties of carbon grains. For the first time it has been pointed out that the intimate structure of a single grain plays a dominant role in extinction processes.

In the present paper we report the results of new experimental analyses, complementary to the UV spectral measurements, performed to study some of the main physical properties of sp^2-based carbons. Attention is also devoted to a careful morphological characterization of the samples. The results demonstrate a strong dependence of the electronic properties on the size of clusters forming the grains.

In § 2 the different experimental lines of attack to the characterization of our samples are described and the results presented. In § 3 the global information coming from the different analyses is discussed to provide a self-consistent framework about the nature of small carbon grains. We believe that this study can be a valuable reference for the understanding of actual properties of carbon-based materials present in space.

2. EXPERIMENTAL ANALYSES AND RESULTS

The production method and thermal processing of the hydrogenated carbon grains (hereafter ACH2) studied in this work are extensively described in previous papers to which we refer the reader for more details (Blanco et al. 1993; Me95). We recall that the ACH2 samples were produced by striking an arc discharge between two amorphous carbon electrodes in hydrogen atmosphere at a pressure of 10 mbar and collected on different substrates at a distance of 5 cm from the source. In the following we present the results obtained by using different analytical techniques in order to characterize in detail our samples.

2.1. C—H *Bonding Configurations*

The first step of the characterization of the ACH2 samples was the evaluation of their hydrogen content. We have already reported (Me95) that the H/C atom ratio, measured by means of microcombustion calorimetry, is 0.62 with an error of about 10%.

Since different carbon hybridizations are possible, it is interesting to understand the actual C—H bonding configuration of our grains. This aspect can be investigated by means of IR spectroscopy. The study of the C—H absorption spectrum has been established to be a quantitative method by comparison with the results from such other techniques as mass spectrometry and nuclear magnetic resonance (Dischler, Bubenzer, & Koidl 1983).

IR transmission measurements of grains deposited onto KBr windows were carried out by using a Fourier transform spectrophotometer (Bruker IFS 66v) with a spectral resolution of 1 cm^{-1}. The normalized C—H stretching spectrum of hydrogenated carbon grains (see Fig. 1) is characterized by a band at 3.03 μm and at least four bands forming the 3.4 μm feature. In order to deconvolve the C—H modes and to evaluate their contribution to the absorption, we performed a Lorentzian line shape fitting analysis of the 3.4 μm band. We obtained the best

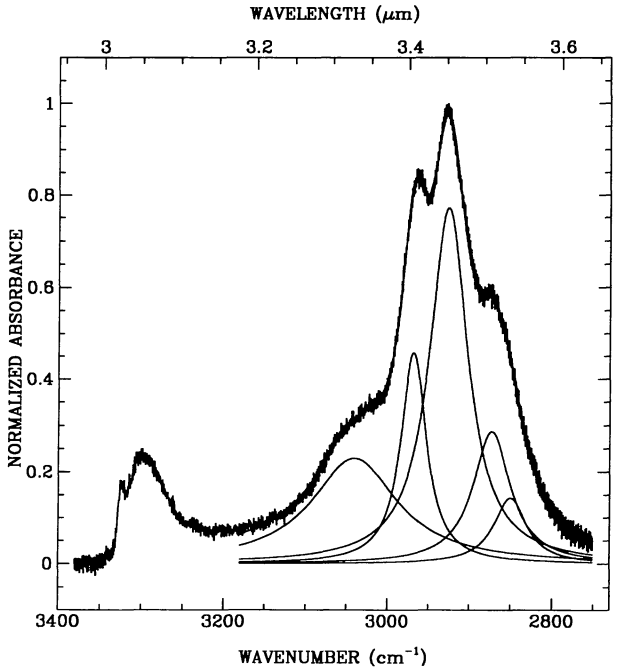

FIG. 1.—The normalized ACH2 absorption spectrum in the C—H stretching region. The deconvolved components obtained by a line shape fitting of the 3.4 μm are also shown. The fitting curve is masked by the noise.

fit by using five Lorentzian oscillators. The fitting curve and the deconvolved components are reported in Figure 1. The modes we found are assigned to various C—H bonding configurations, as shown in Table 1. A complete tabulation of the IR bands of ACH2 is reported by Colangeli et al. (1995).

The analysis of the C—H stretching spectrum demonstrates that (1) three carbon hybridizations are present in the grains and (2) the sp^3 bonding configuration is dominant. In fact, by interpreting the band intensities reported in Table 1 in terms of concentrations, we find that the sp^3/sp^2 ratio is $\simeq 3$.

2.2. *Thermal Annealing of Hydrogenated Grains: Spectral Variations*

The aim of the annealing experiment is twofold: (1) It is a reasonable simulation of carbon grain processing active in space such as UV and cosmic-ray irradiation of small carbon grains (Hecht 1986; Sorrell 1990), and (2) it gives us the opportunity to study systematically the spectral and structural changes in carbon grains due to the hydrogen effusion.

A detailed description of the experiment and the UV spectrum thermal evolution are reported in Me95. Here we briefly summarize the main points of the experimental procedure and the spectral results. We recall that the annealing of ACH2 samples was performed for 3 hr in a microprocessor-controlled cell at a pressure $< 10^{-5}$ mbar. The annealing temperature, T_a, was controlled to better than 1% in the range 250–800°C (see Table 2). A freshly produced sample was used for each annealing process.

The extinction properties of the samples were measured in the range 190–800 nm. For the ACH2 samples and those annealed up to 415°C, the extinction measurements were extended in the extreme-ultraviolet (EUV) down to 40 nm. These spectra are characterized by a strong band, falling at about 93 nm, whose position does not vary with the temperature. A UV band is present in the spectrum of the annealed samples. This feature is not evident in the spectrum of the hydrogenated grains and becomes more intense and shifts toward longer wavelengths as T_a increases. In Figure 2 we report the spectra of grains both as produced and annealed at the highest considered temperature (800°C). The complete thermal evolution of the spectra is reported by Me95 (see their Fig. 1). The dependence of the UV peak position on T_a is shown in Figure 3*a*.

TABLE 1

C—H STRETCH VIBRATIONAL MODES

Mode	Predicted Wavenumber[a] (cm^{-1})	Observed Wavenumber (cm^{-1})	Integrated Intensity (cm^{-1})
sp^1 CH	3305	3300	...
sp^2 CH (aromatic)	3050	3040	40.1
sp^3 CH_3 (asymmetric)	2960	2968	25.8
sp^3 CH_2 (asymmetric)	2925	2926	63.8
sp^3 CH_3 (symmetric)	2870	2873	22.5
sp^3 CH_2 (symmetric)	2855	2850	9.8

[a] From Dischler et al. 1983.

TABLE 2

OPTICAL AND STRUCTURAL PROPERTIES OF THE EXAMINED SAMPLES

T_a[a] (°C)	λ_p[b] (nm)	E_g[c] (eV)	L_a[d] (Å)
...	...	1.34 ± 0.01	6
250	194 ± 2	1.22 ± 0.04	6
325	198 ± 3	1.20 ± 0.02	6
415	214 ± 3	0.92 ± 0.04	8
550	241 ± 2	0.35 ± 0.02	22
600	246 ± 2	0.19 ± 0.03	40
700	252 ± 4	-0.06 ± 0.02	...
800	259 ± 4	-0.13 ± 0.02	...

[a] Annealing temperature.
[b] UV peak position from Mennella et al. 1995a.
[c] Optical gap.
[d] Aromatic coherence length derived from the optical gap.

2.3. *Optical Gap Variations*

As one can note in Figure 2, the spectral changes due to the annealing process involve not only the UV region but also the visual-to-near-IR spectral range. The observed spectral trend is characterized by a broad optical absorption edge, typical of semiconductor materials, which varies with the annealing temperature. The study of this spectral feature provides some of the most valuable data on the structure of amorphous carbons. It is indeed possible to derive the optical gap, E_g, from the absorption edge and then to get information on the degree of clustering of sp^2 sites within the grains. A method for deriving the

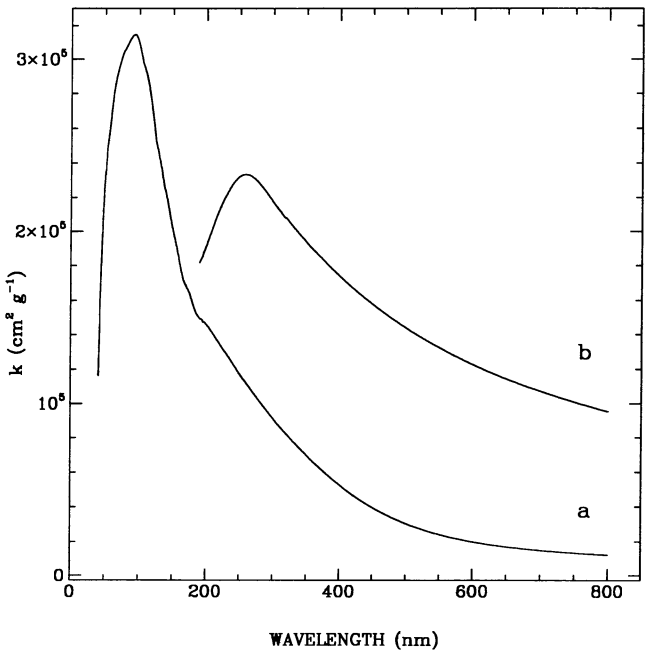

FIG. 2.—Extinction coefficients of hydrogenated amorphous carbon grains as (*a*) produced and (*b*) annealed at 800°C.

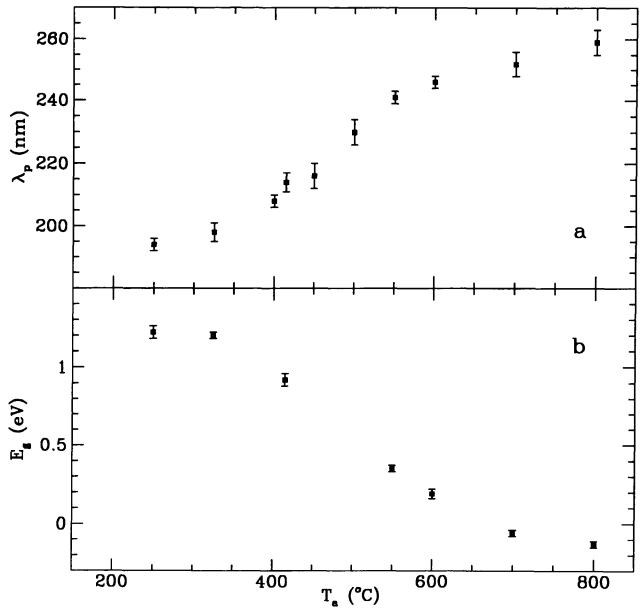

FIG. 3.—The UV peak position (*a*) from Mennella et al. (1995a) and the Tauc gap (*b*) of carbon grains as a function of the annealing temperature. The optical gap for as produced grains is 1.34 eV. The error bars represent the uncertainties determined from repeated experiments on different samples.

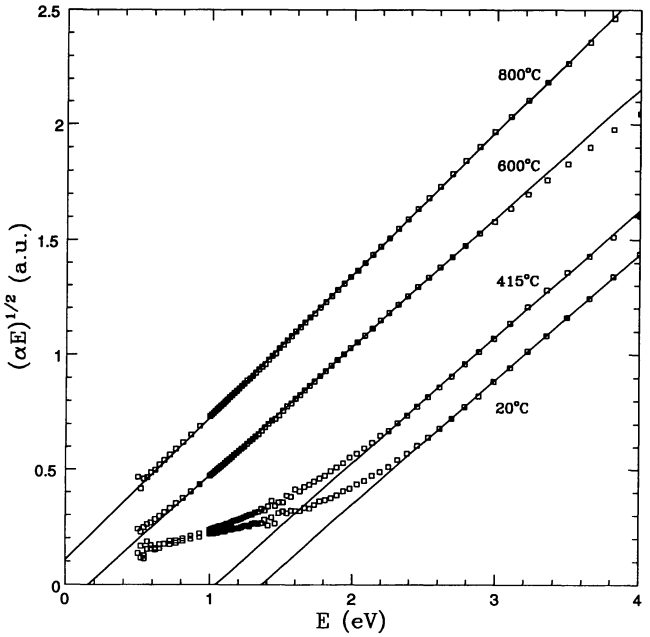

FIG. 4.—Tauc diagram of hydrogenated and annealed carbon grains. The squares represent the experimental points. The fits obtained by means of the Tauc relation (eq. [1] in the text) are also shown. The intersection of the fitting lines with the abscissa axis give the values of the optical gap.

optical gap from optical data is based on the "Tauc relation" between the absorption coefficient, α, and E_g (Tauc, Grigorovici, & Vancu 1966):

$$(\alpha E)^{1/2} = B(E - E_g), \quad (1)$$

where E is the energy and B is a constant. The Tauc relation assumes that density of states (DOS) edges of the valence and conduction band have a parabolic (free electron) form and a constant momentum transition. Although these assumptions may not be fulfilled for all amorphous materials, the Tauc diagram for our samples shows a region in which equation (1) provides a good parameterization of the absorption edge. By extrapolating the linear slope to zero absorption in the Tauc diagram, it is possible to estimate the optical gap (see Fig. 4).

The optical gaps were obtained from spectral measurements repeated on several samples for each considered T_a. The average values, with the corresponding errors, are listed in Table 2. The dependence of E_g on T_a is shown in Figure 3*b*. Starting from a value of 1.34 eV for grains as originally produced, E_g slowly decreases for $T_a < 325$°C; then, a faster decrease is observed in the range 400–600°C. Finally, the closing of the gap takes place at a temperature slightly higher than 600°C.

2.4. *Raman Spectroscopy*

Raman scattering is very sensitive to the structural disorder that breaks the translational symmetry, such as occurs in small crystals. Therefore, Raman spectroscopy is a useful technique for the structural characterization of carbons and provides information about their microstructure.

Raman spectra of the ACH2 and annealed samples were measured in air at room temperature by using a backscattering geometry. The excitation source was the 1064 nm line of a Nd:YAG laser. The power at the sample surface was between 40 and 70 mW. The scattered light was filtered and analysed with a FT spectrophotometer (Bruker IFS 66v) and detected with a LN_2-cooled Ge detector. The spectral resolution was 8 cm^{-1}. The spectra were corrected for the sensitivity of the optical and detection systems by measuring the spectrum of a tungsten lamp of known spectral emissivity.

The thermal evolution of the first-order G and D Raman bands typical of carbon-based materials (see § 3) is shown in Figure 5.

2.5. *Morphological Analysis*

To check any possible modification in the grain morphology during the annealing process, we analyzed the samples by means of electron microscopy. In fact, different aggregation and clumping of the fluffy material might produce variation in the spectral behavior.

The morphological characterization of the hydrogenated and annealed samples was performed by using a field emission scanning electron microscope (SEM 360 FE Cambridge) with maximum resolving power of about 2 nm and magnification up to 500,000 times. We carried out the SEM analysis on the same samples used for UV spectroscopy. The samples were coated with a Cr film, in order to avoid electrical charging of the particles under the electron beam and to increase the signal-to-noise ratio of the images.

As shown in Figure 6*a*, the ACH2 samples are characterized by a chainlike structure of spherical aggregates composed of three to five spherical grains. The average diameter of a single aggregate is 40 nm.

The small-scale structure of the sample was studied by a transmission electron microscope (Philips CM12). The analy-

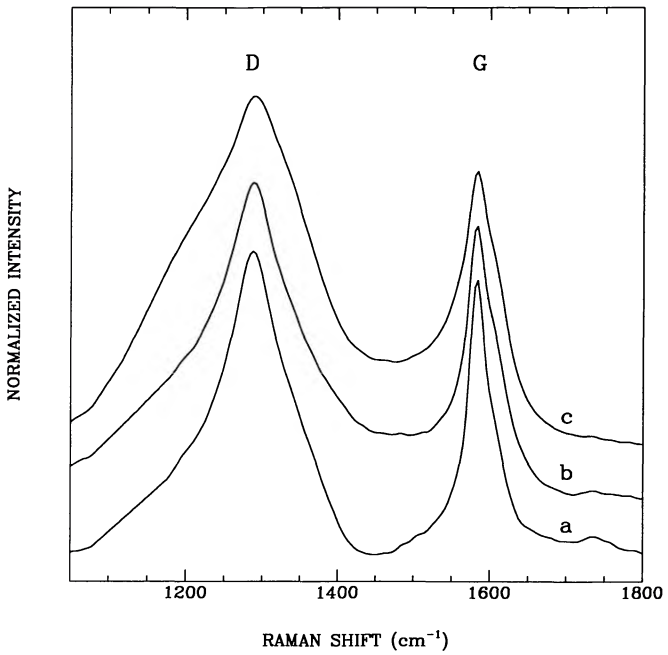

FIG. 5.—First-order G and D Raman bands of carbon grains (*a*) as produced and annealed (*b*) at 600°C and (*c*) at 800°C. The spectra are normalized to the G peak intensity and arbitrarily shifted in ordinate.

sis of TEM images showed that the average diameter of the grains is 11 nm.

SEM images of the unannealed and annealed samples, taken at different magnifications from a large scale down to the dimension of the single aggregate, did not show any significant variation in the morphology (see Fig. 6). Moreover the TEM images showed that the average sizes of single grains do not change after annealing.

3. DISCUSSION

The results reported in the previous section show that important modifications take place in the UV to visual spectrum of hydrogenated amorphous carbon grains because of heat treatment. We found that the spectral variations are correlated to changes of important structural properties. In the following we will propose a self-consistent interpretation of all our data on the thermal evolution of the carbon grains.

As far as morphology is concerned, grain shape, dimension, and clustering degree can affect, in principle, the optical properties of particulate materials (Huffman 1989; Wright 1989; Rouleau & Martin 1991). Therefore, the observed spectral variations could be due to changes of some of these parameters during the annealing. The present SEM and TEM results indicate that all the morphological properties of the samples do not change after the annealing process. Thus, the observed thermal evolution of the UV to visual spectrum of the carbon grains cannot be explained in terms of morphological modifications.

This experimental evidence supports the conclusion drawn by Me95 that the grain internal structure plays a dominant role in the UV extinction processes. The EUV and UV features were assigned, respectively, to $\sigma-\sigma^*$ and $\pi-\pi^*$ electronic transitions of the sp^2 clusters forming the grains, and the shift of the UV peak was interpreted in terms of a progressive dimensional growth of the graphitic islands.

The amorphous carbon analyzed in this work can be considered to be intermediate between diamond, graphite, and hydrocarbon polymers. Noncrystalline carbons can contain variable amounts of sp^2 and sp^3 sites and hydrogen and show physical properties which depend on bond types and on the length scale of the ordered structures. The value of $sp^3/sp^2 \simeq 3$ found for ACH2 grains indicates that their structure is mainly polymeric with an aromatic component which is not negligible. This result is in agreement with the evidence that the presence of hydrogen favors the sp^3 configuration.

The relationship between electronic properties and structure is one of the main physical questions of interest in carbon-based materials. The typical property of the carbon electronic structure is the different behavior of π and σ states. The latter form localized two center bonds which determine the short-range order of the material. The π states can form two center bonds, as in ethylene, or resonant bonds, as in benzene and graphite. In this last case the bonding energy is delocalized, and, therefore, π electrons may introduce medium-range order into the structure.

Thus, for a given fraction of sp^2 and sp^3 sites, the π bonds form graphitic clusters rather than being homogeneously spread through the sample. Robertson & O'Reilly (1987) have indeed shown that the most stable arrangement of sp^2 sites is in compact clusters of aromatic rings. Therefore, the π electrons of sp^2 clusters mainly control the electronic properties of amorphous carbons. Moreover, they determine the optical gap (i.e., the energy spacing between valence and conduction bands) as the edges of electronic DOS are π-like in both hydrogenated and dehydrogenated carbons (Robertson 1986, 1991). Another important feature of π states is that the edges of the π peaks in the electronic DOS are correlated with the graphitic island sizes. According to Robertson (1991), $E_g(eV) \simeq 7.7/L_a(\text{Å})$, where L_a is the aromatic coherence length.

By using the optical gaps of our samples in the previous relation, we obtain that (see Table 2) the cluster sizes do not change up to 325°C, and then a significant increase of L_a, from 8 to 40 Å, is observed in the range 400–600°C. Of course, the Robertson relation gives meaningless cluster sizes for very small E_g values. It seems now more evident that, during the thermal annealing of our samples, the hydrogen loss produces changes in the structure (the clustering degree increases) and, consequently, in the electronic properties. The delocalization of the π bonding increases, and a complete aromatization occurs for $T_a > 600$°C, as evidenced by the optical gap closing at around this temperature. Moreover, new microcombustion calorimetry measurements did not detect hydrogen in the samples annealed at 600°C (Trkula 1994). Therefore, a complete aromatization of the bonding is expected for $T_a > 600$°C.

The previous evolution is in agreement with that of hydrogenated amorphous carbon (a-C:H) films. In fact, Dischler et al. (1983) found that the sp^2 fraction in a-C:H films reaches almost 100% after the annealing at 600°C, where $E_g = 0$. Moreover, Fink et al. (1984) noted a delocalization of π electrons between 400°C and 600°C with the closing of the gap at the highest edge of this range. Similarly, Smith (1984) obtained $E_g = 0$ at 650°C.

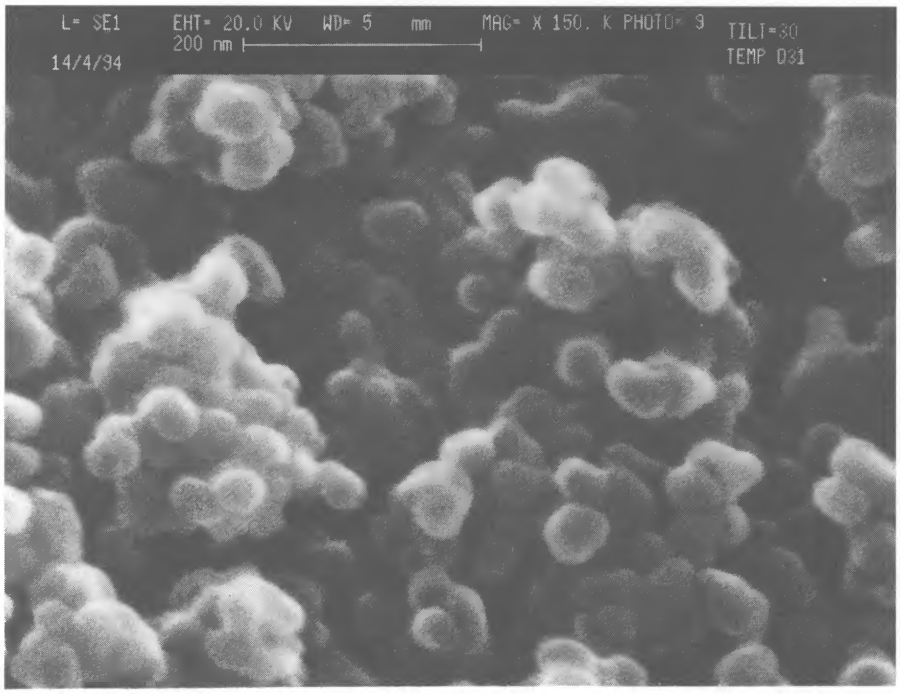

FIG. 6*a*

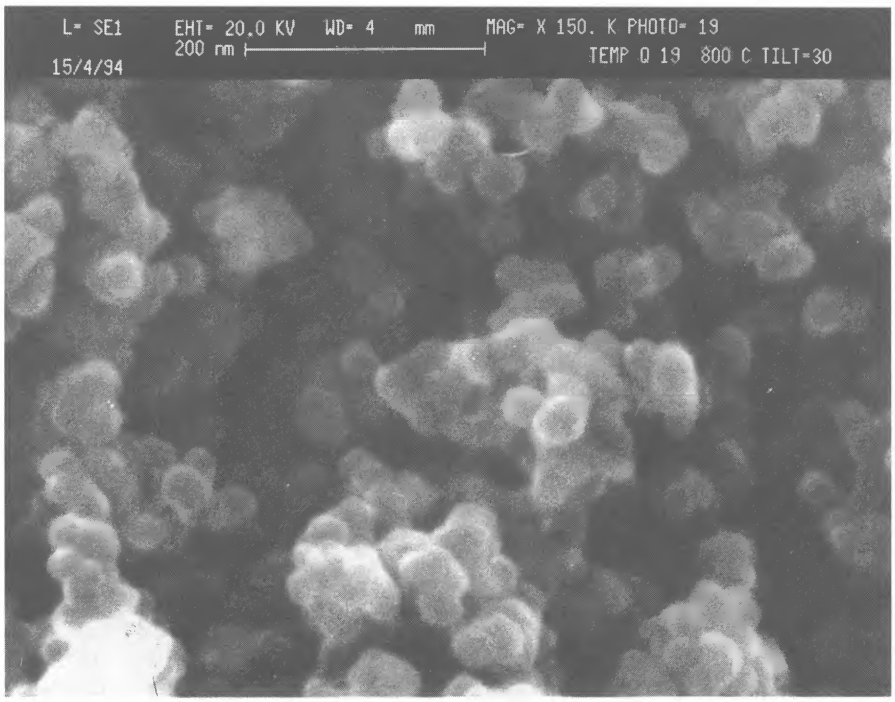

FIG. 6*b*

FIG. 6.—SEM micrographs of grains (*a*) as produced and (*b*) after annealing at 800°C

It is worthwhile noting that the L_a values reported in Table 2 refer to the larger clusters present within the grains. Robertson & O'Reilly (1987) have estimated that when clusters of different sizes are present, the observed gap is controlled by the largest clusters, present at a concentration of a few percent. The observed broad absorption edges (Fig. 2) indicate that a cluster size distribution is present within our carbon grains. A very sharp edge should be observed if the absorption were due to clusters of a single size.

The clustering degree within the grains can explain the

different spectral behavior of hydrogenated and annealed samples (see Fig. 2). The absorption is determined by the number of sp^2 clusters and their dimensions: for hydrogenated grains, a few clusters should be present, and their sizes should be very small, with the largest clusters having a size of 6 Å. On the other hand, for the grains annealed at 800°C the aromatic clusters grow in number and sizes: the largest islands are able to close the gap. Therefore, their absorption is stronger than that produced by hydrogenated grains.

The behaviors of the UV peak position, λ_p, and E_g as a function of T_a suggest a correlation between these two parameters. The plot of λ_p versus E_g is reported in Figure 7. The linear correlation coefficient is -0.994, and the best-fit straight line of experimental data is $\lambda_p(\mathrm{nm}) = 253.3 - 45.8 \times E_g(\mathrm{eV})$. Since E_g is inversely proportional to L_a, the previous result implies that the π transition energy depends on the sp^2 cluster size. We recall that, for one-electron interband transitions, the absorption depends on both the dipole matrix momentum between the valence and conduction bands and on the joint density of states of these bands, $J(E)$. Since Robertson did not find a strong dependence of $J(E)$ on the clustering degree, we interpret the correlation between λ_p and E_g as an evidence of the dependence of the π transition dipole matrix momentum on the sp^2 cluster size: matrix element effects emphasize lower energy π transitions in large clusters and higher energy transitions in small clusters.

The validity of the correlation between λ_p and E_g is confirmed by the values obtained for carbon grains produced by arc discharge in argon atmosphere and annealed in the range 250–780°C and by burning benzene in air (Mennella et al. 1995b). Our result does not account for the empirical relation found by Koike, Kaito, & Shibai (1994) for carbonaceous materials, between the UV peak position and the graphitic microcrystallite size as determined by high-resolution TEM: the peak shifts toward longer wavelengths as the microcrystallite size decreases.

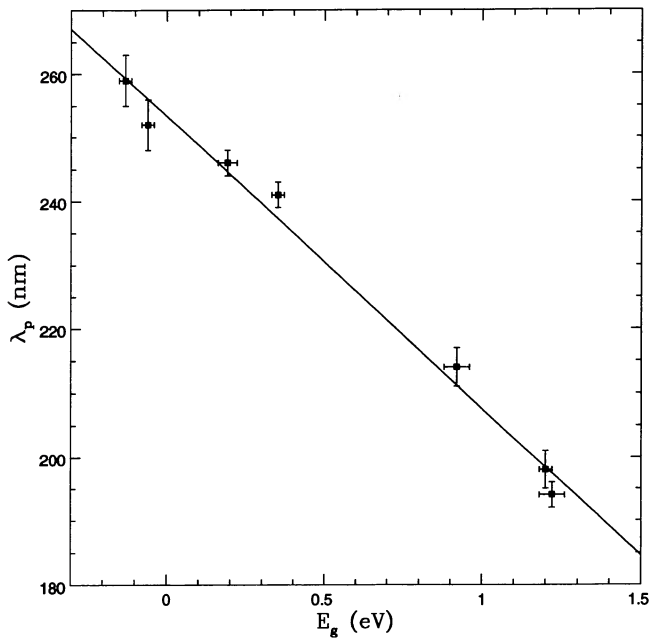

FIG. 7.—The UV peak position vs. the optical gap. The straight line represents the best fit of the data.

In the framework of the discussion reported above, a relevant role can be played by Raman spectroscopy, as it allows us to estimate the cluster dimension by means of anhelastic scattering measurements. We recall that the reference of any analysis of sp^2-bonded carbons is the graphite lattice. The first-order Raman spectrum of both large single crystals of graphite and of highly oriented pyrolytic graphite (HOPG) shows the G band at 1582 cm^{-1} (Nemanich & Solin 1979). A second Raman active mode falls at such a low frequency (42 cm^{-1}) that is is hard to resolve from the Rayleigh scattering.

For small graphite crystallites and disordered carbons the wavevector selection rule, $\boldsymbol{k} = \boldsymbol{0}$, is relaxed so that the peaks present in the phononic DOS may appear in the Raman spectrum and determine important spectral modifications to the Raman spectrum of graphite (Nemanich & Solin 1979; Lespade, Al-Jishi, & Dresselhan 1982; Mennella et al. 1995c). The most characteristic band of disordered carbon falls at about 1300 cm^{-1} (D line). It has been attributed to an in-plane A_{1g} mode, silent for infinite graphitic layer, which becomes active on the boundary of small crystallites as stressed by Tuinstra & Koenig (1970). These authors found that the D and G lines' intensity ratio, Γ, is $\propto 1/L_a$ for polycrystalline graphite. Actually, this relation fails for very small cluster sizes: the D band intensity cannot increase indefinitely at low L_a, as it is bounded above by the phononic DOS corresponding to the mode as noted by Tamor et al. (1989) and by Robertson (1991). These authors suggested that Γ versus L_a increases for $L_a < 12$ Å and decreases for $L_a > 12$ Å; it is only in the latter range that the relation by Tuinstra & Koenig is valid. A similar behavior was reported by Dillon, Woollam, & Kathanant (1984) for the thermal evolution of Γ in annealed a-C:H films. They found a maximum of Γ for $L_a = 16$ Å.

The intensity ratio Γ measured for our samples as a function of the annealing temperature is shown in Figure 8. Γ increases for T_a up to 600°C and then decreases for higher T_a. According to the previous discussion we can tentatively assume $L_a \simeq 14$ Å for the sample annealed at 600°C. This result is not in contrast with $L_a = 40$ Å deduced from the optical gap because, as already mentioned, that value refers to the largest sp^2 clusters, while the Raman spectroscopy is sensitive to their average sizes. At present, we cannot apply the Tuinstra & Koenig relation to estimate the cluster sizes from the Γ values in the range $L_a > 14$ Å because of the resonant Raman effect in carbons. The discussion of this phenomenon is beyond the scope of this paper (for a detailed discussion, see, e.g., Wagner et al. 1989). We simply recall that Γ depends on the laser wavelength used to obtain Raman spectra of carbonaceous materials. Tuinstra & Koenig (1970) derived Γ by exciting their samples at 488 nm, while we used an excitation at 1064 nm. Work is in progress to measure the resonant behavior of our samples.

4. CONCLUSIONS

The results obtained by thermally processing submicron hydrogenated amorphous carbon grains evidence an evolution of their structural properties in terms of sp^2 cluster growth in number and size. This evolution is driven by the hydrogen loss.

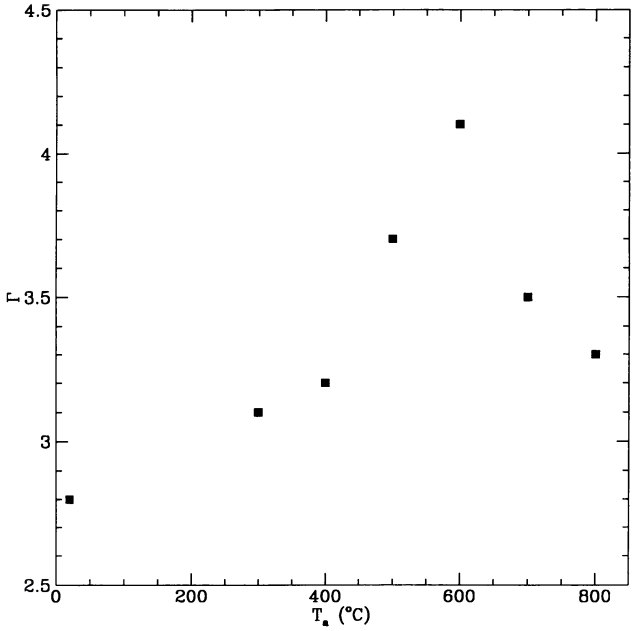

FIG. 8.—Thermal evolution of the integrated intensity ratio of the D and G Raman bands.

Hydrogen in the starting grains (H/C atom ratio = 0.62) favors the sp^3 bonding configuration. The sp^2 site arrangement is in compact clusters of fused aromatic rings, and only small clusters exist (largest size $\simeq 6$ Å). Despite the evidence that only $\simeq$30% of sites are sp^2, a substantial degree of clustering is present.

The structure of the grains significantly changes as the annealing temperature increases. Only a small increase of the largest clusters is observed up to $\simeq$400°C. On the other hand, since Me95 reported a significant hydrogen content reduction in the samples annealed at 400°C (H/C atom ratio = 0.22), an increase in number, rather than in size, of the graphitic islands should take place in this temperature range. This conclusion is supported by the slight increase of the Γ ratio in Raman spectra, which indeed demonstrates a growth in the number of the clusters interacting with the laser beam (Dillon et al. 1984).

More important structural modifications occur in the range 400–600°C. At the highest edge of this interval the hydrogen is completely removed from the samples (H/C atom ratio $\simeq 0$). A substantial growth in cluster size is observed, and a complete π bond delocalization takes place. A further dimensional growth of the clusters is expected for temperature greater than 600°C, as evidenced by the Γ behavior.

The structural evolution causes deep variations in the electronic properties, which in turn determine the observed spectral changes in the extinction coefficient. In particular, the interpretation of the UV shift toward longer wavelengths in terms of sp^2 cluster size growth, proposed by Me95, is confirmed by optical gap and Raman measurements. Actually, we found a basic correlation between UV peak position and optical gap, which is interpreted as a dependence of the dipole matrix momentum of π transitions on the sp^2 cluster size.

Finally, we would like to point out that it is not our aim to claim that the carbon grains we studied are the actual carriers of the 217.5 nm feature. Nevertheless, we believe that assessing electronic and structural properties of cosmic analogs, as done in this work, can help to solve the puzzling problem of the interstellar extinction bump. In the models proposed so far to interpret this feature, homogeneous particles with different shapes, dimensions, and coatings have been considered, and, very often, the optical properties of bulk graphite have been used. Our results suggest that the interaction of electromagnetic radiation with carbon grains, having dimensions comparable with those expected for the carriers of the bump, is very sensitive to the internal structure of grains, so that more attention should be paid to the careful analysis of the intimate nature of carbonaceous carriers in the simulation of the interstellar extinction bump.

M. Trkula and J. R. Stephens are warmly thanked for the microcombustion calorimetry measurements performed at Los Alamos National Laboratory. We thank G. Cafiero for performing TEM measurements and S. Inarta, N. Staiano, and E. Zona for their technical assistance during the measurements. This work has been supported by ASI, CNR, and MURST research contracts.

REFERENCES

Blanco, A., Bussoletti, E., Colangeli, L., Fonti, S., Mennella, V., & Stephens, J. R. 1993, ApJ, 406, 739
Blanco, A., Bussoletti, E., Colangeli, L., Fonti, S., & Stephens, J. R. 1991, ApJ, 382, L97
Bussoletti, E., Colangeli, L., Borghesi, A., & Orofino, V. 1987, A&AS, 70, 257
Colangeli, L., Mennella, V., Palumbo, P., Rotundi, A., & Bussoletti, E. 1995, A&AS, in press
Czyzak, S. J., & Santiago, J. J. 1973, Ap&SS, 23, 443
Dillon, R. O., Woollam, J. A., & Katkanant, V. 1984, Phys. Rev. B, 29, 3482
Dischler, B., Bubenzer, A., & Koidl, P. 1983, Solid State Comm., 48, 105
Donn, B., Hecht, J. H., Khanna, R., Nuth, J., Stranz, D., & Anderson, A. B. 1981, Surface Sci., 106, 576
Draine, B. T. 1989, in Interstellar Dust, ed. L. J. Allamandola & A. G. G. M. Tielens (Dordrecht: Kluwer), 313
Draine, B. T., & Malhotra, S. 1993, ApJ, 414, 632
Fink, J., Müller-Heinzerling, T., Pflüger, J., Scheeler, B., Dischler, B., Koidl, P., Bubenzer, A., & Sah, R. E. 1984, Phys. Rev. B, 30, 4713
Fitzpatrick, E. L., & Massa, D. 1986, ApJ, 307, 286
———. 1988, ApJ, 328, 734
Hecht, J. H. 1986, ApJ, 305, 817
Hecht, J. H., Holm, A. V., Donn, B., & Wu, C. C. 1984, ApJ, 280, 228
Huffman, D. R. 1989, in Interstellar Dust, ed. L. J. Allamandola & A. G. G. M. Tielens (Dordrecht: Kluwer), 329
Koike, C., Kaito, C., & Shibai, H. 1994, MNRAS, 268, 321
Lespade, P., Al-Jishi, R., & Dresselhau, M. S. 1982, Carbon, 20, 427
Mathis, J. S. 1994, ApJ, 422, 176
Mathis, J. S., & Whiffen, G. 1989, ApJ, 341, 808
Mennella, V., Colangeli, L., Blanco, A., Bussoletti, E., Fonti, S., Palumbo, P., & Mertins, H. C. 1995a, ApJ, 444, 288 (Me95)
Mennella, V., Colangeli, L., Bussoletti, E., Merluzzi, P., Monaco, G., Palumbo, P., & Rotundi, A. 1995b, Planet. Space Sci., in press

Mennella, V., Monaco, G., Colangeli, L., & Bussoletti, E. 1995c, Carbon, 33, 115
Muci, A. M., Blanco, A., Fonti, S., & Orofino, V. 1994, ApJ, 436, 831
Nemanich, R. J., & Solin, S. A. 1979, Phys. Rev. B, 20, 392
Robertson, J. 1986, Adv. Phys., 35, 317
———. 1991, Prog. Solid State Chem., 21, 199
Robertson, J., & O'Reilly, E. P. 1987, Phys. Rev. B, 35, 2946
Rouleau, F., & Martin, P. G. 1991, ApJ, 377, 526
Smith, F. S. J. 1984, Appl. Phys., 55, 764
Sorrell, W. H. 1990, MNRAS, 243, 570
Tamor, M. A., Haire, J. A., Wu, C. H., & Hass, K. C. 1989, Appl. Phys. Lett., 54, 123
Tauc, J., Grigorovici, R., & Vancu, A. 1966, Phys. Status Solidi, 15, 627
Trkula, M. 1994, private communication
Tuinstra, F., & Koenig, J. L. 1970, J. Chem. Phys., 53, 23
Wagner, J., Ramsteiner, M., Wild, Ch., & Koidl, P. 1989, Phys. Rev. B, 40, 1817
Witt, A. N., Walker, G. A. H., Bohlin, R. C., & Stecher, T. P. 1982, ApJ, 261, 492
Wright, E. L. 1989, ApJ, 346, L89